PAPER • **OPEN ACCESS**

Real-time wireless signal processing for contactless heart rate monitoring with impulse-radio ultra-wideband radar technology

To cite this article: Siti Mahfuzah Fauzi *et al* 2026 *Biomed. Phys. Eng. Express* **12** 015028

Biomedical Physics & Engineering Express

OPEN ACCESS

RECEIVED
19 November 2024

REVISED
13 August 2025

ACCEPTED FOR PUBLICATION
28 October 2025

PUBLISHED
18 December 2025

PAPER

Real-time wireless signal processing for contactless heart rate monitoring with impulse-radio ultra-wideband radar technology

Siti Mahfuzah Fauzi[1,2], **Latifah Munirah Kamarudin**[1,3,4,*] and **Tiu Ting Yii**[5]

[1] Faculty of Intelligent Computing, Universiti Malaysia Perlis, Perlis, Malaysia
[2] Integrated Graduate School of Medicine, Engineering & Agricultural Sciences, University of Yamanashi, Kofu, Japan
[3] Faculty of Engineering, Graduate Faculty of Interdisciplinary Research, University of Yamanashi, Kofu, Japan
[4] Centre of Excellence for Advanced Sensor Technology (CEASTech), Universiti Malaysia Perlis, Perlis, Malaysia
[5] Faculty of Electronic Engineering & Technology, Universiti Malaysia Perlis, Perlis, Malaysia
[*] Author to whom any correspondence should be addressed.

E-mail: sitimahfuzah@studentmail.unimap.edu.my, latifahmunirah@unimap.edu.my and s211022106@studentmail.unimap.edu.my

Keywords: IR-UWB, wireless heart rate detection, non-contact, FIR Kaiser window, FFT, autocorrelation, peak finding with moving average filter

Abstract

Impulse-radio ultra-wideband (IR-UWB) radar technology employs short-duration impulse waves with broad bandwidth for precise detection and tracking, offering a cost-effective, non-invasive alternative for portable heart rate monitoring. Its practical design supports long-term healthcare applications without adverse effects. However, effective implementation necessitates robust signal processing techniques to minimize interference from clutter signals and breathing harmonics, enabling the extraction of the target signal from background noise and interference. This study aims to provide real-time measurements through the implementation of signal processing algorithms such as Fast Fourier Transform (FFT), autocorrelation, and peak finding with a moving average filter (MAF) to extract heartbeat signals from background noise and interference. Algorithms were tuned for range parameters and bandpass filter order, with a Kaiser window-based FIR filter (order 250) selected for testing. The FFT algorithm achieved the highest accuracy of 85.6%, while peak finding with MAF and autocorrelation attained accuracies of 78.5% and 76.6%, respectively. The FFT algorithm demonstrated superior potential for real-time heart rate monitoring and was implemented in a graphical user interface (GUI) for data visualization.

1. Introduction

The impulse-radio ultra-wideband (IR-UWB) radar technology gives rise to non-contact heart rate monitoring by emitting and recording radar waves that detect tiny chest movements causes by cardiac activity. In contrast to conventional electrocardiogram (ECG) and pulse oximeters, radar-based monitoring mitigates hygiene hazards, improves patient comfort, and facilitates continuous, long-term monitoring in clinical and home environments [1]. To guarantee reliable readings, signal processing methods are used to reduce noise and interference while retrieving critical physiological data. Key elements such as the subject's location, measurement angle, and movement have a substantial impact on data dependability. The radar readings are then analyzed using powerful algorithms that separate heartbeat signals from background noise and breathing harmonics. This technology allows for real-time, high-precision heart rate monitoring without physical limits, making it suited for use in clinical, home-based, and remote healthcare settings. By removing the requirement for physical touch, IR-UWB radar offers a viable option for continuous and unobtrusive physiological monitoring, hence enhancing patient comfort and long-term usage.

2. Literature review

2.1. Fundamental of radar technology in non-contact heart rate monitoring

Non-contact heart rate monitoring with radar technology is a refined technique that allows heart rate measurement without making physical touch [2]. Radar technologies such as IR-UWB [3], Frequency-Modulated Continuous Wave (FMCW) [4], and

Doppler [5] radars have been extensively researched and demonstrated efficacy for this application. Radar technology acts by producing radio waves that reflect off a target and return as an echo, enabling the detection of movement, even slight chest motion due to heartbeat and breathing [6, 7]. Research has consistently shown that radar accurately detects heartbeats without direct skin contact, positioning it as a viable non-invasive option [2, 7, 8]. In contrast to traditional sensors, radar enables uninterrupted monitoring without requiring electrodes, hence reducing the hazards of skin irritation and infection transmission [2]. This functionality is especially beneficial in critical care, newborn surveillance, sleep assessments, and home healthcare applications [9]. Furthermore, radar technology diminishes the necessity for frequent inspections and alleviates the challenges associated with treating infectious illnesses like COVID-19. It is increasingly utilized in remote monitoring for chronic cardiovascular illnesses, Alzheimer's, and dementia care [10].

Among radar technologies, IR-UWB radar is particularly valued because to its excellent signal-to-noise ratio (SNR) and ability to give exact, real-time heart rate readings even with body movement [2, 11]. Unlike FMCW and Doppler radar, IR-UWB offers higher precision in detecting heart motion while successfully filtering out breathing harmonics and external noise. Its contactless nature makes it extremely ideal for continuous monitoring in both medical and daily situations [1, 3]. With its benefits in accuracy, non-contact capabilities, and real-time monitoring, IR-UWB radar provides a dependable alternative to current heart rate monitoring approaches.

2.2. Signal processing techniques

Higher-Order Harmonics Peak Selection (HOHPS) [8] is a signal processing approach that improves the accuracy and reliability of heart rate measurements, even in the presence of breathing and ambient noise. The experimental findings demonstrate that the proposed approach has an average mean absolute error (MAE) of 1.32. The peak selection algorithm is a critical component of the HOHPS approaches, as it picks the higher-order harmonic peaks of the radar signal to accurately estimate the heart rate.

Assume array P has entries $p_1, p_2, \ldots p_n$, indicating all peaks over 100 beats per minute (BPM). The algorithm then discovers all peaks p_i between 100 and 400 BPM and saves their associated frequencies in a vector, as illustrated in equation (1):

$$P = [p_1\ p_2 \cdots\ p_n] \tag{1}$$

The subsequent step is to estimate two initial values for the heart rate, as given in equation (2):

$$HR_{guess} = \begin{bmatrix} hr_{guess1} \\ hr_{guess2} \end{bmatrix} \tag{2}$$

If p_1 and p_2 differ by less than 100 BPM, p_1 and p_2 are considered the first two harmonics of the heart rate and are divided by 2 and 3, respectively, to produce the initial heart rate assumptions hr_{guess1} and hr_{guess2}. If the difference between p_1 and p_2 is 100 BPM or larger, p_1 is considered the initial fundamental value for the heart rate, hr_{guess1} and p_2 is presumed to be the second harmonic and divided by 2 to obtain hr_{guess2}.

The vector P is divided by hr_{guess1} and hr_{guess2} individually, and the results are rounded to obtain the integer multiple arrays $\mathrm{Int1_{mul}}$ and $\mathrm{Int2_{mul}}$, as indicated in equation (3) and (4).

$$\begin{aligned} Int_{mul} &= round\left([p^T p^T] \times \begin{bmatrix} \frac{1}{hr_{guess1}} & 0 \\ 0 & \frac{1}{hr_{guess2}} \end{bmatrix} \right) \\ &= [int1_{mul}\ \ int2_{mul}] \end{aligned} \tag{3}$$

where

$$\begin{aligned} int1_{mul} &= [int1_{mul1}\ \ int1_{mul2}\ \ \ldots\ \ int1_{muln}]^T, \\ int2_{mul} &= [int2_{mul1}\ \ int2_{mul2}\ \ \ldots\ \ int2_{muln}]^T. \end{aligned} \tag{4}$$

After that, vector P is divided element-wise by $\mathrm{Int1_{mul}}$ and $\mathrm{Int2_{mul}}$ separately to create heart rate estimation arrays $hr1_{est}$ and $hr2_{est}$ as given in equations (5) and (6).

$$\begin{aligned} hr_{est} &= \frac{[p^T p^T]}{[int1_{mul}\ \ int2_{mul}]} \\ &= [hr1_{est}\ \ hr2_{est}] \end{aligned} \tag{5}$$

where

$$\begin{aligned} hr1_{est} &= [hr1_{est1}\ \ hr1_{est2}\ \ \ldots\ \ hr1_{estn}], \\ hr2_{est} &= [hr2_{est1}\ \ hr2_{est2}\ \ \ldots\ \ hr2_{estn}]. \end{aligned} \tag{6}$$

To calculate $error1$ and $error2$, deduct hr_{guess1} and hr_{guess2} from $hr1_{est}$ and $hr2_{est}$, respectively, as illustrated in equations (7) and (8).

$$\begin{aligned} Error &= abs\left(\begin{bmatrix} hr1_{est} & hr2_{est} \end{bmatrix} - \begin{bmatrix} hr_{guess1} & hr_{guess2} \end{bmatrix} \right) \\ &= [error1\ \ error2], \end{aligned} \tag{7}$$

where

$$\begin{aligned} error1 &= [error1_1\ \ error1_2\ \ \ldots\ \ error1_n], \\ error2 &= [error2_1\ \ error2_2\ \ \ldots\ \ error2_n]. \end{aligned} \tag{8}$$

If the estimated errors surpass a 6 BPM threshold, the resulting high-frequency peak is deemed noise. The estimated heart rates and errors connected with this peak are deleted from the heart rate estimation array depending on their index.

The averages of the remaining errors for $error1$ and $error2$ are determined. hr_{slt} represents the predicted heart rate array with the lowest average inaccuracy. Equation (9) shows that the final heart rate, hr_{est} is calculated by averaging hr_{slt}.

$$hr_{est} = mean\ (hr_{slt}), \tag{9}$$

where

$$hr_{slt} = \begin{cases} hr1_{est}\ , & if\ mean\ (error1) \leqslant mean\ (error2) \\ hr2_{est}, & \text{otherwise} \end{cases} \tag{10}$$

Other strategies include using the lowpass Butterworth filter in research that focus on human movement and vital sign extraction [12–14]. This filter effectively reduces high-frequency noise from the received radar signals, improving the clarity of vital information. As mentioned in [15], the magnitude response of the lowpass Butterworth filter is given by equation (11), while the attenuation is defined by equation (12).

$$|H(\omega)|^2 = \frac{1}{1 + \left(\frac{\omega}{\omega_c}\right)^{2N}} \tag{11}$$

Attenuation

$$A = -10\ log\left(1 + \left(\frac{\omega}{\omega_c}\right)^{2N}\right) \tag{12}$$

The non-linearity of radar signals presents breathing harmonics, notably the second and fourth harmonics, which overlap with the human heart rate range. To overcome this problem, a Notch filter bank technique is utilized to eliminate breathing harmonics, setting notch frequencies at 2 to 4 times the extracted breathing frequency before heart rate estimation [16]. The Kalman filter is another noise-reduction method used in signal processing. In [1], it was utilized for vital sign monitoring at distances of 1 m and 2 m. Results demonstrated an increase in signal-to-noise ratio (SNR), with values increasing to 18.2 dB at 1 m and 14.9 dB at 2 m after filtering. This modification resulted to a reduction in root mean square error (RMSE) to 0.840 and 1.831, respectively, illustrating its usefulness in enhancing heart rate measurement accuracy.

For multi-person detection in low SNR situations, the Channel Impulse Response (CIR) Smoothing Spline (CIR-SS) method [17] is applied. This approach delivers great penetration, exact range measuring, minimal power consumption, and cost efficiency. The program gathers radar echoes, performs thresholding, and does time-of-arrival (TOA) range estimate to detect several individuals' vital signs. Additional processing, including clutter reduction and azimuth estimation, boosts accuracy in retrieving heart rate data. Experimental assessments demonstrate that CIR-SS efficiently separates heartbeats from breathing signals, even in complicated situations such as through-wall monitoring. The system obtained breathing and heart rate estimate errors of 5.14% and 4.87%, respectively. Studies [4, 17] employing X4M200 IR-UWB radar proved the accuracy of CIR-SS for non-contact multi-person heart rate monitoring.

Another research [5] studied single-channel Doppler radar with an enhanced signal processing method for heart rate detection. It featured a Finite Impulse Response (FIR) filter to minimize noise and retrieve heart rate information. Three methods—Fast Fourier Transform (FFT), autocorrelation, and peak detection with a moving average filter (MAF)—were utilized for heart rate estimate. Among them, peak detection obtained the lowest mean difference of 2.6 BPM compared to reference values, followed by FFT (3.5 BPM) and autocorrelation (5.1 BPM). The standard deviation data further confirmed peak detection as the most accurate approach.

Based on the literature presented above, this study aims to improve heart rate estimation accuracy using IR-UWB radar by investigating, adapting, and optimizing signal processing techniques including FFT, autocorrelation, and peak selection for radar-based heart rate monitoring. Each method is evaluated using real datasets collected in a hospital setting at a fixed range. To further assess robustness, the proposed method is also tested using datasets acquired in a controlled environment across multiple distances to examine the impact of range on performance. The contributions of this study are as follows:

1. Independent implementation and fine-tuning of FFT, autocorrelation, and peak selection algorithms specifically for IR-UWB radar.
2. Integration of the optimized method into a real-time monitoring system with a graphical user interface (GUI) displaying heart rate, and time-stamps for clinical and remote health applications.

3. Methodology

This study employs PyCharm, an integrated development environment (IDE) for Python, developed by JetBrains, to process GUI of the real-time heart rate monitoring using the X4M200 radar sensor, developed by Novelda AS. The X4M200 is a radar sensor System-on-Chip (SoC) designed primarily for breathing monitoring and its sensitivity is adjustable from 0 to 9, where higher values increase sensitivity. The sensor operates in the 6.0–8.5 GHz ultra-wideband range, with a center frequency of 7.29 GHz. It uses a built-in noise map to filter out background noise and improve detection accuracy, providing respiration waveforms, movement levels, and presence detection signals [18].

Before further processing, the X4M200 generates raw received radar signals in the form of a radar scattering matrix. The sensor is configured to acquire scans (frames) at a rate of 20 frames per second (FPS), generating a radar scattering matrix in which each row represents spatial samples from different range

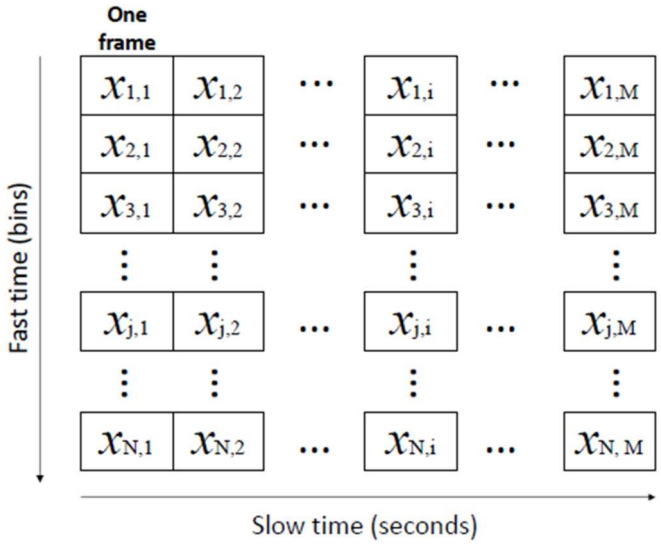

Figure 1. Radar scattering matrix.

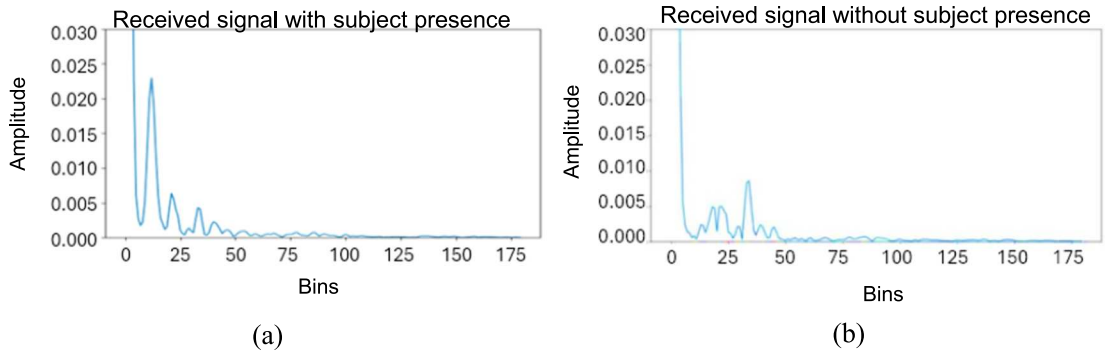

Figure 2. Received signal (a) with (b) without subject presence.

bins (fast time), and each column represents observations (frames) recorded at various time intervals (slow time). Figure 1 illustrates the resulting radar scattering matrix [19]. The range resolution of the sensor is approximately 5.14 cm, meaning it can differentiate objects separated by at least this distance [18]. The amplitude of the received signal is influenced by target reflectivity, motion, clutter and multipath interference. The raw signal contains both direct reflections and secondary multipath components, which can introduce unwanted artifacts. Additionally, motion artifacts from breathing and environmental noise are present in the signal, requiring appropriate filtering and signal processing techniques to accurately extract heart-related micro-movements [20]. The tested algorithms are responsible for isolating heart-related signals from these unwanted components, ensuring accurate heart rate estimation.

3.1. Signal visualization

Figure 2(a) shows the graph of the UWB received signal in baseband form when a subject is present and close to the radar, while figure 2(b) depicts the graph when no subject is in the radar sensing area. The received signal will change according to the chest movements for the subject breathing, as illustrated in figures 3(a) and (b) showing the inhaling and exhaling phases, respectively. The heartbeat movement cannot be observed in these figures as clearly as the breathing movement, since the chest movement for the heartbeat is too small. Therefore, the signal must undergo signal processing techniques specifically for heartbeat detection to remove clutter signals and breathing harmonics.

3.2. Datasets and experimental setup

This study utilizes two types of datasets. The first dataset comprises data collected at UiTM hospital using the X4M200 IR-UWB radar, as described in paper [21]. Signal processing is conducted using data collected over 10-minute intervals from this recorded dataset, primarily aimed at validating the proposed signal processing technique.

The second dataset is data in real-time application using the setup as presented in figure 4. The experiment will be conducted in a controlled indoor

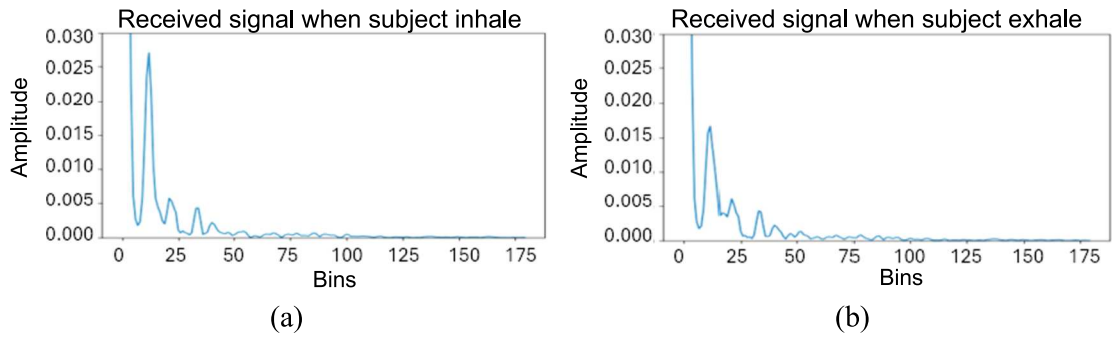

Figure 3. Received signal when subject (a) inhale (b) exhale.

Figure 4. Experiment setup.

environment to ensure consistent conditions with 2 healthy subjects for data recording in approximately 3 min for each participant. The subjects will maintain a sitting posture with normal breath. Data collection will be performed in front directions to capture comprehensive information at different ranges from the subjects, specifically at 50 cm, 100 cm, 150 cm, and 200 cm. This variation aims to investigate the effect of proximity on the accuracy of heart rate detection using radar technology and the sensing area of the radar. Heart rates extracted from the data with the three algorithms were compared with the reference data taken using a pulse oximeter.

3.3. Development of signal processing algorithm

The collected data are processed using a Kaiser window FIR filter for clutter signal reduction, followed by testing three different methods; FFT, autocorrelation, and peak finding with MAF to detect the heart rate signal. Each algorithm are tested with different parameters for the FIR window, including filter order and passband cutoff frequencies, through a trial-and-error method tailored for optimal use with IR-UWB in diverse experimental setups. The heart rate determined by the algorithms was compared with wrist pulse oximeter, Nonin 3150. Subsequently, the optimal parameter configuration for the algorithm will be applied to real-world data to evaluate its performance and adjust for variability, aiming for consistent and accurate heart rate monitoring.

3.3.1. FIR kaiser window

The Kaiser window-based FIR filter is applied to remove noise and interference from the raw radar signal. By setting appropriate cutoff frequencies, it isolates the heart signal by filtering out the low-frequency breathing signals and other high-frequency noise. This process ensures that only the frequency components corresponding to heartbeats are retained in the signal for further processing. This filter is a versatile digital signal processing tool that is a superior choice for accurate and reliable heart rate detection using radar technology. It is highly effective in reducing noise and unwanted components from signals, making it suitable for heart rate detection in radar applications [22–24]. It provides superior performance in filtering compared to other window functions like Blackman, Bartlett, and Hanning,

Table 1. Filter parameters for kaiser window-based bandpass filtering.

FIR kaiser bandpass filter	FIR equiripple
Frequency specifications	$f_L = 0.5$ Hz, $f_H = 8.5$ Hz
Beta, β	5
Filter taps	201
Filter order, N	50, 100, 150, 200, 250

particularly in radar digital signal processing [25, 26]. For radar heart rate detection, the Kaiser window function is highly effective at clutter signal removal. It excels in noise reduction [26], provides low amplitude error [27], supports both real-time and offline analysis [22], enhances SNR, and benefits from parameter optimization [23].

The Kaiser window is employed to design the filter coefficients using the windowing method, influencing the frequency response.

$$Y(n) = \sum_{k=0}^{M} h(k) \cdot X(n-k) \tag{13}$$

Equation (13) represents the convolution operation, where $Y(n)$ is the output signal, $X(n-k)$ is the input signal, shifted by k time steps, and $h(k)$ are the FIR filter coefficients [28]. The Kaiser window provides significant flexibility in designing FIR filters by allowing control over the trade-off between the main-lobe width and side-lobe attenuation. In this study, the filter order was fine-tuned across five different values to determine the optimal configuration for heart rate estimation. The filter specifications are detailed in table 1.

3.3.2. FFT

FFT calculates the N frequency spectra corresponding to these N time domain signals. N spectra are synthesized into a single frequency spectrum. DFT equation as below:

$$X[k] = \sum_{n=0}^{N-1} x[n] W_N^{nk} \quad for\ 0 \leqslant k \leqslant N-1 \tag{14}$$

where $n = 0,\ldots,N\text{-}1$ is signal index, $k = 0,\ldots,N\text{-}1$ is spectrum index. $x[n]$ is be real and complex number and W_N is phase factor and it is a complex number [29].

By analyzing the frequency spectrum, the algorithm identifies the peak frequency, which corresponds to the heart rate. The highest peak in the FFT output is used to determine the heart rate in BPM.

3.3.3. Autocorrelation

Autocorrelation, also known as serial correlation, is the correlation of a signal with a delay copy of itself as a function of delay. In other words, similarity exists between the observations of the same subject at separate times, and it is a function of time lag. The analysis of autocorrelation is a mathematical tool for finding repeating patterns, such as to find a periodic signal obscured by noise.

The autocorrelation coefficient, $\rho_x(\tau)$ denotes the correlating degree of the same event between two different periods, and the expression is as equation (15):

$$\rho_x(\tau) = E[(x_i - \mu)(x_{i+\tau} - \mu)]\,\mu)(x_{i+\tau} - \mu)] \tag{15}$$

where τ is the interval between series i_{th} and $(i+\tau)_{th}$, E is the expected value operator, μ is the mean value of the series x and σ is the deviation of x [30].

Autocorrelation is performed with a lag ranging from 1 to 200 samples. It measures how the signal correlates with itself over various time lags. The first significant peak in the autocorrelation function indicates the signal's periodicity, which corresponds to the heart rate. By identifying the lag at which this peak occurs, the heart rate is estimated.

3.3.4. Peak finding with moving average filter

Before applying the Moving Average Filter (MAF), the signal is first clipped to remove any sudden spikes or outliers. The clipping threshold is calculated as the mean of the absolute values of all samples in the filtered signal. This threshold is used to limit both positive and negative amplitudes, effectively reducing the influence of extreme values that could distort the signal.

Once the signal is clipped, the next step is to smooth it using a MAF as the remaining noise component in the received signal might affect the efficiency in peak detection [31]. A simple moving average with a window size of 60 is used, as defined in equation (16):

$$\bar{Z}_k = \frac{\sum_{i=k-(s-1)}^{i=k} Z_i}{s} \tag{16}$$

Where $\bar{Z}_k$ is the averaged value at index k of the sequence Z, Z_i is the individual elements and s represents the window size, determining the influence of the previous data on the current observation. The MAF helps reduce high-frequency noise, providing a smoother waveform that is more suitable for accurate peak detection. Peaks are identified by evaluating each sample to determine if it is a local maximum within a 90-sample window. The total number of peaks detected within the specified time duration is then counted, and the heart rate is estimated in BPM.

3.4. Evaluation metric

The performance of the tested algorithms in heart rate estimation is evaluated based on accuracy. Accuracy is determined by calculating the proportion of correctly detected instances, including both positive and negative cases, relative to the total number of instances [32]. It is calculated using the following formula:

Table 2. Average accuracy for 10-minute data interval using hospital UiTM dataset (A). Subject 1 (B). Subject 2 (C). Subject 3 (D). Subject 4 (E). Subject 5.

BPF order	50	100	150	200	250
Algorithm	Average accuracy for 10-min data intervals (%)				
			(A)		
FFT	38.90	39.50	48.30	51.80	68.90
Autocorrelation	No data	No data	27.50	81.00	74.80
Peak finding with MAF	88.80	92.10	87.30	87.30	**91.50**[a]
			(B)		
FFT	36.90	51.70	56.20	64.60	75.20
Autocorrelation	No data	No data	49.30	63.90	**77.00**[a]
Peak finding with MAF	42.70	47.50	45.30	54.40	55.60
			(C)		
FFT	39.00	26.50	51.50	53.80	66.30
Autocorrelation	No data	No data	21.50	78.00	77.90
Peak finding with MAF	79.10	83.80	83.00	86.40	**90.30**[a]
			(D)		
FFT	33.90	43.00	49.80	61.00	69.70
Autocorrelation	No data	No data	58.10	47.00	56.50
Peak finding with MAF	54.40	57.60	68.10	73.00	**77.90**[a]
			(E)		
FFT	43.30	44.00	39.50	45.10	78.80
Autocorrelation	No data	No data	41.40	67.50	67.60
Peak finding with MAF	77.00	70.60	77.40	80.70	**84.50**[a]

[a]Bold indicates the highest accuracy achieved with the BPF of order 250 across 5 subjects.

$$Accuracy\ (\%) = \frac{true\ value - measured\ value}{true\ value} \times 100 \tag{17}$$

The average accuracy is then calculated over a N-minute data interval to ensure a reliable performance assessment.

4. Result

Before implementing the algorithms for real-time monitoring, we first evaluated their performance on a dataset collected from a hospital at UiTM. This testing phase served as a benchmark to assess the algorithms' accuracy prior to their application in real-time scenarios. These algorithms were tested on five different datasets.

Table 2 lists the accuracy of the heart rates of the five subjects. It can be seen that the autocorrelation does not show heart rate for BPF order below 150. Autocorrelation relies on identifying repeated patterns over time, which may not exist in the signal data at those distances. FFT analyzes frequency content, while peak finding with MAF identifies peaks based on amplitude, which might still be detectable even if autocorrelation fails. The highest accuracy for the three algorithms—FFT, autocorrelation, and peak finding with MAF—was achieved using a Kaiser window-based FIR filter with a bandpass cutoff frequency of 0.5 Hz to 8.5 Hz and a filter order of 250.

Based on table 2, the highest accuracy rates for FFT, autocorrelation, and peak finding with a MAF, are 91.50%, 77%, 90.30%, 77.90%, and 84.50% respectively. The accuracy of these algorithms is limited because the datasets include subjects with low heart rate (below 50 BPM), normal heart rate (between 50 to 90 BPM), and high heart rate (above 90 BPM). These three algorithms can achieve high accuracy when the heart rate reading in normal range, but the accuracy drops for subjects with high and low heart rate. This could be due to the filter's cutoff frequency, as low and high heartbeats theoretically have lower or higher frequencies, respectively. Thus, the current cutoff frequency bandpass may be more suitable for normal heartbeats. To validate this situation, the algorithm was applied to real-time data for heart rate detection.

Next, the algorithms were tested using real-time data across four ranges: 50 cm, 100 cm, 150 cm, and 200 cm. Subject 1's detection accuracy, shown in figure 5, was below 90%, likely due to their elevated heart rate (above 90 BPM). In contrast, Subject 2's accuracy, depicted in figure 6, was higher due to their heart rate falling within the normal range. While the FFT algorithm showed better performance for detecting high heart rates, autocorrelation and peak finding with MAF were more accurate for normal heart rates. Based on

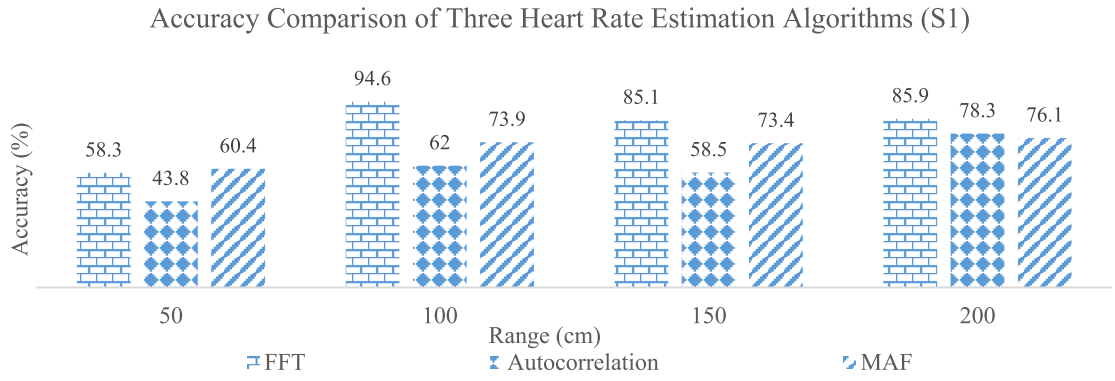

Figure 5. Average accuracy of Subject 1 with high heart rate.

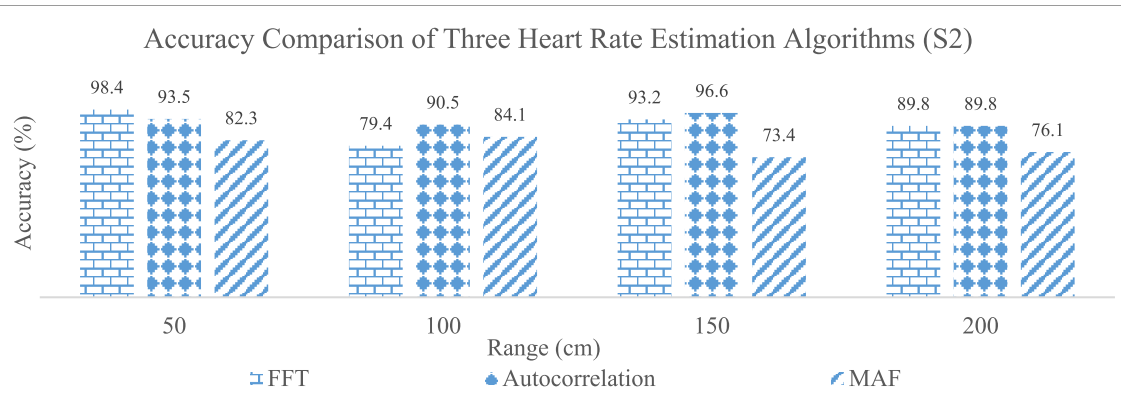

Figure 6. Average accuracy of Subject 2 with normal heart rate.

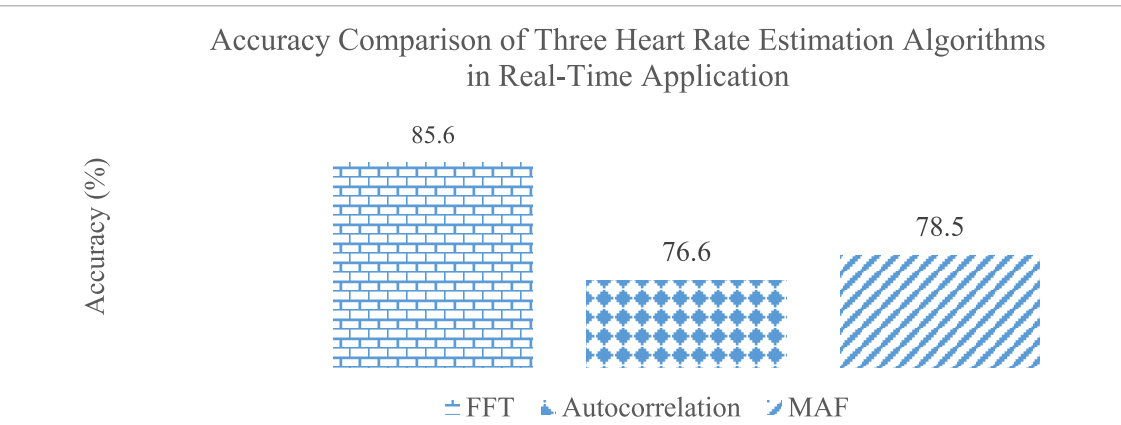

Figure 7. Average accuracy in real-time application.

figures 5 and 6, certain methods achieve over 90% accuracy within the range of 50 cm to 150 cm, although performance varies depending on the method and measurement distance. These findings indicate that increasing the measurement range can adversely affect the detection of weak radar heartbeat signals [33].

Figure 7 presents the average accuracy of the algorithms at different measurement distances. The FFT algorithm demonstrates the highest average accuracy at 85.6% and is therefore incorporated into the GUI for real-time data visualization, as shown in figure 8. This superior performance is likely due to FFT's robustness in extracting frequency components from radar heartbeat signals, making it well-suited for practical heart rate monitoring. The peak finding method with MAF and the autocorrelation method achieved average accuracies of 78.5% and 76.6%, respectively, and remain available options within the system. The algorithm selection in the GUI can be dynamically adjusted according to performance requirements or environmental conditions. Future work includes further optimizing these algorithms and exploring hybrid approaches to enhance accuracy and reliability across diverse operating ranges.

Figure 8. Data visualization in GUI.

5. Conclusion

The X4M200 IR-UWB radar is a low-power, health-safe device intended for long-term healthcare monitoring. It determines heart rate by collecting chest movements related to breathing and heartbeat through reflected radar signals. However, its implementation employing FFT within a GUI has limitations, with accuracy falling short of the 95% target. Optimizing signal processing techniques and settings is required to boost performance and adaptability to varied situations.

One key difficulty is inaccuracy when persons move out of the radar's detecting region. In such instances, the system may maintain a steady BPM output instead of recognizing the subject's absence. The present 5-second FIFO update constantly analyzes heart rate frames, however if the subject departs the detection zone, BPM values might change until remain constant (e.g., from 69 BPM to 60 BPM) instead of reaching 0 BPM. This occurs because the algorithm chooses the largest variance signal, which might be an ambient reflection rather than an actual heart rate. An error-handling technique is needed to identify true heart rate data from deceptive high-variance reflections.

Despite the promising capabilities of the proposed system, there are several limitations that need to be addressed. Firstly, the system operates under the assumption that the detected individual remains still. Any movement can introduce signal distortions, which may reduce the accuracy of the heart rate estimation. Additionally, radar signals are susceptible to reflections from surrounding objects, which can lead to incorrect readings and interference in heart rate measurement. Another limitation is the system's performance in environments with multiple people. The algorithm is currently designed to detect the heart rate of a single individual, and when multiple people are present within the sensing area, it may struggle to differentiate between their heart rates, affecting the overall reliability of the system. Moreover, the adaptive bandpass filtering mechanism in the system must dynamically adjust to account for actual heart rate variations. A fixed bandpass range may not effectively accommodate physiological differences across individuals, leading to potential inaccuracies in the heart rate estimation.

To address these limitations, incorporating predictive tracking and adaptive filtering techniques could enhance system reliability, particularly when subjects temporarily leave the sensing area. Furthermore, refining the algorithm to better distinguish multiple simultaneous heartbeats would improve the system's applicability in medical and crowded environments. Real-world challenges such as motion artifacts and breathing harmonics further complicate accurate heart rate estimation. Therefore, expanding the study to include more subjects and optimizing algorithm parameters are essential steps toward improving robustness, validating results, and ultimately enhancing estimation accuracy in practical settings.

Acknowledgments

The authors thank the UiTM Research Ethics Committee (Ref. number: REC/07/2021 (FB/37)) for providing the data and the Malaysian Ministry of Higher Education (MoHE) for funding this work through Fundamental Research Grant Scheme (FRGS): FRGS/1/2018/SKK06/UNIMAP/02/1.

Conflict of interest statement

The authors declare that they have no conflicts of interest related to this work.

Data availability statement

The data cannot be made publicly available upon publication because they contain sensitive personal information. The data that support the findings of this study are available upon reasonable request from the authors.

Ethical statement

This study was conducted in accordance with the principles embodied in the Declaration of Helsinki and in compliance with local statutory requirements. Ethical approval for this research was obtained from the UiTM Research Ethics Committee (Reference Number: REC/07/2021 (FB/37)). All participants provided written informed consent to participate in the study, ensuring that their rights and privacy were protected. The data collected during this research contain sensitive personal information and are kept secure and confidential in accordance with the agreed terms with the participants.

Author contributions

Siti Mahfuzah Fauzi 0009-0000-7343-0413
Conceptualization (equal), Formal analysis (equal), Validation (equal), Visualization (equal), Writing – original draft (equal), Writing – review & editing (lead)

Latifah Munirah Kamarudin 0000-0002-2547-3934
Conceptualization (equal), Formal analysis (equal), Funding acquisition (lead), Project administration (lead), Resources (lead), Supervision (equal), Validation (equal)

Tiu Ting Yii
Conceptualization (equal), Data curation (equal), Formal analysis (equal), Investigation (equal), Methodology (equal), Software (equal), Validation (equal), Visualization (equal), Writing – original draft (equal)

References

[1] Khan F and Cho S H 2017 A detailed algorithm for vital sign monitoring of a stationary/non-stationary human through IR-UWB radar *Sensors* **17** 290
[2] Lee Y *et al* 2018 A novel non-contact heart rate monitor using impulse-radio ultra-wideband (IR-UWB) radar technology *Sci. Rep.* **8** 13053
[3] Zhang X, Yang X, Ding Y, Wang Y, Zhou J and Zhang L 2021 Contactless simultaneous breathing and heart rate detections in physical activity using IR-UWB radars *Sensors* **21** 5503
[4] Dong X, Feng Y, Cui C and Lu J 2023 CEEMDAN-ICA-based radar monitoring of adjacent multi-target vital signs *Electronics* **12** 2732
[5] Sameera J N, Droitcour A D and Boric-Lubecke O 2022 Heart rate detection using single-channel Doppler radar system *Proc. of the Annual Int. Conf. of the IEEE Engineering in Medicine and Biology Society, EMBS* pp 1953–6
[6] Aardal Ø 2013 Radar monitoring of heartbeats and respiration *Ph.D. thesis* University of Oslo, Faculty of Mathematics and Natural Sciences
[7] Iwata Y, Thanh H T, Sun G and Ishibashi K 2021 High accuracy heartbeat detection from CW-doppler radar using singular value decomposition and matched filter *Sensors* **21** 3588
[8] Xu H *et al* 2021 Accurate heart rate and respiration rate detection based on a higher-order harmonics peak selection method using radar non-contact sensors *Sensors 2022* **22** 83
[9] Monitoring Vital Signs with Radar Technology 2024 https://urad.es/en/aplicaciones/monitorizacion-de-signos-vitales/
[10] Ullah R, Dong Y, Arslan T and Chandran S 2023 A machine learning-based classification method for monitoring alzheimer's disease using electromagnetic radar data *IEEE Trans. Microw Theory Tech.* **71** 4012–26
[11] Wang D, Yoo S and Cho S H 2020 Experimental comparison of IR-UWB radar and FMCW radar for vital signs *Sensors* **20** 6695
[12] Dang X, Zhang J and Hao Z 2022 A non-contact detection method for multi-person vital signs based on IR-UWB radar *Sensors* **22** 6116
[13] Cao L, Wei R, Zhao Z, Wang D and Fu C 2023 A novel frequency-tracking algorithm for noncontact vital sign monitoring *IEEE Sens. J.* **23** 23044–57
[14] Choi S H and Yoon H 2023 Convolutional neural networks for the real-time monitoring of vital signs based on impulse radio ultrawide-band radar during sleep *Sensors* **23**
[15] Rexy J, Velmani P and Rajakumar T C Heart beat peak detection using signal filtering in ECG data *International Journal of Advanced Technology and Engineering Exploration* **6** 2394–7454
[16] Xiang M, Ren W, Li W, Xue Z and Jiang X 2022 High-precision vital signs monitoring method using a FMCW millimeter-wave sensor *Sensors* **22** 7543
[17] Wu S, Tan K, Xia Z, Chen J, Meng S and Guangyou F 2016 Improved human respiration detection method via ultra-wideband radar in through-wall or other similar conditions *IET Radar Sonar Navig.* **10** 468–76
[18] Novelda A S 2017 *B Preliminary - X4M200 Datasheet* 10–2 www.xethru.com
[19] Maitre J, Bouchard K, Bertuglia C and Gaboury S 2021 Recognizing activities of daily living from UWB radars and deep learning *Expert Syst. Appl.* **164**
[20] Cheraghinia M *et al* 2024 'A comprehensive overview on UWB radar: applications, standards *Signal Processing Techniques, Datasets, Radio Chips, Trends and Future Research Directions* (https://doi.org/10.48550/arXiv.2402.05649)
[21] Husaini M *et al* 2022 Non-contact breathing monitoring using sleep breathing detection algorithm (SBDA) based on UWB radar sensors *Sensors* **22** 5249
[22] Seydnejad S R and Kitney R I 1997 Real-time heart rate variability extraction using the Kaiser window *IEEE Trans. Biomed. Eng.* **44** 990–1005
[23] Das P, Naskar S K and Patra S N 2017 An approach to enhance performance of Kaiser window based filter *Proc. - 2016 2nd IEEE Int. Conf. on Research in Computational Intelligence and Communication Networks, ICRCICN 2016* pp 256–61
[24] Jadhav S, Pooja B, Asawari C and Namrata C 2017 FPGA based ECG Signal noise suppression using windowing techniques *International Journal of Engineering Trends and Technology* **47** 505–8
[25] Sulistyaningsih *et al* 2019 Performance comparison of blackman, bartlett, hanning, and kaiser window for radar digital signal processing *4th International Conference on Information Technology, Information Systems and Electrical Engineering, ICITISEE* pp 391–4

[26] Melgoza C M et al 2020 Comparing radar receiver pulse deinterleaving performance of differing window functions for bandpass FIR filter design *11th Annual IEEE Information Technology, Electronics and Mobile Communication Conference, IEMCON* pp 505–10
[27] Li C and An Q 2020 Harmonic detection algorithm based on kaiser window *IEEE Conference on Telecommunications, Optics and Computer Science, TOCS* pp 60–3
[28] Mbachu C B, Onoh G N, Idigo V E, Ifeagwu E N and Nnebe S U 2011 Processing ECG signal with Kaiser Window-based FIR digital filters *International Journal of Engineering Science and Technology* **3** 6775–83
[29] Gasmi A 2022 *What is Fast Fourier Transform?* Société Francophone de Nutrithérapie et de Nutrigénétique Appliquée https://hal.archives-ouvertes.fr/hal-03741810
[30] Shen H et al 2018 Respiration and heartbeat rates measurement based on autocorrelation using IR-UWB radar *IEEE Trans. Circuits Syst. Express Briefs* **65** 1470–4
[31] Liu J, Gao Z, Li Y, Lv S, Liu J and Yang C 2024 Ranging offset calibration and moving average filter enhanced reliable UWB Positioning in classic user environments *Remote Sens.* **16** 2511
[32] Powers D M W 2011 Evaluation: from precision, recall and F-measure to ROC, informedness, markedness and correlation *International Journal of Machine Learning Technology* **2** 37–63
[33] Al-Masri E and Momin M 2018 Detecting heart rate variability using millimeter-wave radar technology *Proc. - 2018 IEEE Int. Conf. on Big Data, Big Data* pp 5282–4